MicroRNA172 controls inflorescence meristem size through regulation of APETALA2 in Arabidopsis

Qing Sang[1]* (iD), Alice Vayssières[1]* (iD), Diarmuid S. Ó'Maoiléidigh[1,2] (iD), Xia Yang[1] (iD), Coral Vincent[1] (iD), Enric Bertran Garcia de Olalla[1] (iD), Martina Cerise[1] (iD), Rainer Franzen[1] and George Coupland[1] (iD)

[1]Department of Plant Developmental Biology, Max Planck Institute for Plant Breeding Research, Cologne 50829, Germany; [2]Institute of Systems, Integrative, and Molecular Biology, University of Liverpool, Liverpool, L69 7ZB, UK

Author for correspondence:
George Coupland
Email: coupland@mpipz.mpg.de

Summary

- The APETALA2 (AP2) transcription factor regulates flower development, floral transition and shoot apical meristem (SAM) maintenance in Arabidopsis. *AP2* is also regulated at the post-transcriptional level by microRNA172 (miR172), but the contribution of this to SAM maintenance is poorly understood.
- We generated transgenic plants carrying a form of *AP2* that is resistant to miR172 (rAP2) or carrying a wild-type *AP2* susceptible to miR172. Phenotypic and genetic analyses were performed on these lines and *mir172* mutants to study the role of *AP2* regulation by miR172 on meristem size and the rate of flower production.
- We found that *rAP2* enlarges the inflorescence meristem by increasing cell size and cell number. Misexpression of *rAP2* from heterologous promoters showed that *AP2* acts in the central zone (CZ) and organizing center (OC) to increase SAM size. Furthermore, we found that AP2 is negatively regulated by AUXIN RESPONSE FACTOR 3 (ARF3). However, genetic analyses indicated that ARF3 also influences SAM size and flower production rate independently of AP2.
- The study identifies miR172/AP2 as a regulatory module controlling inflorescence meristem size and suggests that transcriptional regulation of *AP2* by ARF3 fine-tunes SAM size determination.

Introduction

In vascular plants, the formation of above-ground organs such as leaves and flowers is dependent on the activity of shoot apical meristems (SAMs) (Holt *et al.*, 2014). Within the SAM, the maintenance of a stem cell population is balanced with the depletion of pluripotent cells that are displaced towards the meristem periphery and differentiate (Laux, 2003). This balance is responsible for the continuous production of organs and the maintenance of SAM size. During crop domestication, selection for increased meristem size has occurred together with breeding for elevated seed production and enlarged fruits (Kitagawa & Jackson, 2019). Moreover, recent studies demonstrated a positive correlation between SAM size and flower or seed production in Arabidopsis and crops (Je *et al.*, 2016; Serrano-Mislata *et al.*, 2017; Landrein *et al.*, 2018). Therefore, regulation of SAM size may contribute to the improvement of crop yield and fitness in natural populations.

The SAM is multilayered and can be divided into different zones. The central zone (CZ) encompasses three clonally distinct cell layers (L1–L3) and is characterized by slowly dividing cells, whereas the peripheral zone (PZ) surrounding the CZ is characterized by rapidly dividing cells (Satina *et al.*, 1940). Cells within the CZ maintain stem cell identity, whereas those in the PZ are recruited for differentiation into lateral organs (Meyerowitz, 1997). Stem cells in the CZ must be replenished to facilitate plant growth, although excessive stem cell proliferation also alters plant growth patterns (Clark *et al.*, 1993, 1995). The organizing center (OC) is located beneath the CZ but also partially overlaps with it and is marked by the expression of *WUSCHEL* (*WUS*), which encodes a homeodomain transcription factor (Mayer *et al.*, 1998). The WUS protein is mobile and moves into the stem cells, where it directly promotes the expression of *CLAVATA3* (*CLV3*), a marker of stem cell identity (Fletcher *et al.*, 1999). *CLV3* encodes a small extracellular peptide that binds to and modifies the activity of complexes of membrane-localized receptor complexes, thereby restricting *WUS* expression to the OC (Clark *et al.*, 1997; Stone *et al.*, 1998; Fletcher *et al.*, 1999; Rojo *et al.*, 2002; Lenhard & Laux, 2003). Disruption of this feedback loop between *WUS* and *CLV3* activity results in dramatic changes in meristem size and plant growth (Carles & Fletcher, 2003).

The morphology and function of the SAM change during the transition from vegetative to reproductive development. During vegetative growth of Arabidopsis, leaf primordia are formed on the flanks of the SAM, whereas floral transition involves the

---

*These authors contributed equally to this work.

change in identity of the SAM into an inflorescence meristem that forms secondary inflorescences and flowers. Floral transition also involves a considerable increase in the size of the Arabidopsis SAM, a phenomenon called doming, which includes an increase in meristem height (Jacqmard *et al.*, 2003; Kinoshita *et al.*, 2020). Pathways that control flowering time also contribute to the increase in meristem size during the doming (Kinoshita *et al.*, 2020). In Arabidopsis, some members of the APETALA2-LIKE (AP2-LIKE) transcription factor family are key regulators of flowering time (Yant *et al.*, 2010). The simultaneous inactivation of all six *AP2-LIKE* genes – *AP2, TARGET OF EAT1* (*TOE1*), *TOE2, TOE3, SCHNARCHZAPFEN* (*SNZ*) and *SCHLAFMÜTZE* (*SMZ*) – results in very early flowering (Yant *et al.*, 2010), whereas overexpression of most of these genes causes late flowering (Aukerman & Sakai, 2003; Schmid *et al.*, 2003; Chen, 2004; Jung *et al.*, 2007; Mathieu *et al.*, 2009; Zhang *et al.*, 2015). The mRNA of each of these genes is targeted by microRNA172 (miR172), which in Arabidopsis is encoded by five *MIR172* genes (Rhoades *et al.*, 2002). Overexpression of miR172 or its depletion also results in early- or late-flowering plants, respectively (Chen, 2004; Lian *et al.*, 2021; Ó'Maoiléidigh *et al.*, 2021).

Moreover, *AP2* increases the size of shoot and floral meristems, although how this is mediated is unclear (Chen, 2004; Würschum *et al.*, 2006). Recently, the SAM of plants lacking the activity of all five *MIR172* genes was found to be enlarged (Lian *et al.*, 2021), but whether this was due to increased activity of *AP2* or to other *AP2-LIKE* genes was not examined. Ectopic expression of *AP2* results in indeterminate flowers and, in this context, *AP2* was proposed to be a direct negative regulator of *AUXIN RESPONSE FACTOR 3* (*ARF3*, also known as *ETTIN*) (Chen, 2004; Liu *et al.*, 2014). ARF3 also directly negatively regulates *AP2*, which suggests that AP2 and ARF3 are components in a double-negative feedback loop (Simonini *et al.*, 2017). However, most of these experiments were performed using whole inflorescences, so it remains unclear whether the interactions between *AP2* and *ARF3* are relevant in the SAM.

To further understand how AP2 and miR172 control SAM size, we uncoupled the activity of *AP2* from miR172 by generating a fluorescently tagged miR172-resistant form of *AP2* (*rAP2-VENUS*) that was expressed from its endogenous regulatory sequences and analyzed *mir172* mutants. We also used heterologous promoters to test where in the meristem rAP2 controls meristem size, and explored the relationship between AP2 and ARF3 in regulating SAM size. Our data demonstrate the importance of miR172 regulation of AP2 in the CZ and OC in controlling meristem size and flower production.

Materials and Methods

Plant materials, growth conditions and phenotypic analysis

Arabidopsis thaliana Columbia (Col-0) ecotype was used as the wild-type for all experiments. The mutant alleles *ap2-12* (Yant *et al.*, 2010), *mir172abd, mir172abd ap2-12, mir172abcde*, (Ó'Maoiléidigh *et al.*, 2021) and *arf3-2* (Okushima *et al.*, 2005), and reporter lines *pAP2::AP2-VENUS* (Ó'Maoiléidigh *et al.*,

2021) have been described previously. Plants were grown in conditions with long days (LDs; 16 h : 8 h, light : dark) or short days (SDs; 8 h : 16 h, light : dark). Shoot apices were harvested at time points that spanned the floral transition (12, 15, 18 and 21 LDs) or at the 1-cm-bolting stage, when the main inflorescence stem had reached a height of 1 cm. For most genotypes, time to flowering was scored on the day the first flowers opened. However, flowers of *ap2-12* mutants opened prematurely, so the size of the flowers and the pistil length were considered to ensure that the first flowers were fully mature.

Plasmid construction and plant transformation

The *AP2* locus was cloned by polymerase incomplete primer extension (PIPE; Klock & Lesley, 2009), with modifications for large fragments and multiple inserts. All PCR amplifications were performed using Phusion Enzyme (New England BioLabs, Frankfurt am Main, Germany) following the manufacturer's recommendations. The *AP2* coding sequence was amplified from genomic DNA and cloned into pDONR207 (Invitrogen) by BP reaction to generate *csAP2-pDONR207*. To create *rAP2*, site-directed mutagenesis was performed to alter the nucleotide sequence of the miRNA172-binding site within *AP2* (Chen, 2004), using *csAP2-pDONR207* as a template and primers containing the desired mutations in the miRNA172-binding site (Supporting Information Fig. S1a). The gene sequence of the VENUS fluorescent protein (Nagai *et al.*, 2002) was amplified and a linker of nine alanine codons was added to obtain an amplicon of 772 nucleotides (9AV) to create insertion-PIPE (I-PIPE). Vector-PIPE was generated using *cs(r)AP2-pDONR207* as a template, to generate a PCR fragment of 5.3 kb. A 1 : 10 mixture of I-PIPE and vector-PIPE was transformed into *Escherichia coli* (*E. coli*) DH5-α cells (Chung *et al.*, 1989). The PCR product was digested with *Dpn*I (New England BioLabs) and used to transform *E. coli* DH5a cells. The *rAP2(-VENUS)-pDONR207* plasmid was sequenced to confirm the presence of the desired constructs. Similarly, a 7.7 kb PCR product of the *AP2* promoter as I-PIPE was amplified and vector-PIPE was generated using *cs(r)AP2(-VENUS)-pDONR207* as a template. The final constructs, *pAP2::(r)AP2(-VENUS)-pDONR207*, were verified by digestion and sequencing. The same method was used to fuse *rAP2-VENUS* to different promoters: *pWUS* (6.3 kb), *pCLV3* (4 kb), *pAtML1* (6.3 kb), *pHMG* (2.8 kb) and *pFD* (4.3 kb). The primers used are listed in Table S1. Col-0 plants were transformed by floral dipping (Clough & Bent, 1998). Transformants were selected by spraying twice with 200 µg ml^{-1} ammonium-glufosinate (Bayer Crop Science, Monheim am Rhein, Germany). Homozygous plants carrying a single insertion of the transgene were selected on Murashige & Skoog medium (Murashige & Skoog, 1962) containing 1% sucrose and 10 µg ml^{-1} phosphinotricin.

RNA extraction, real-time quantitative PCR and RNA-sequencing

Total RNA from apical meristem-enriched tissue was extracted using the RNeasy Plant Mini Kit (Qiagen) and treated with

RNase-free DNase I (Ambion). cDNA was synthesized using a Superscript IV First Strand Synthesis System (Invitrogen). Transcript expression was quantified by quantitative reverse transcription polymerase chain reaction (RT-qPCR) with the SYBR Green Supermix (Bio-Rad) using a CFX384 Touch Real-Time PCR Detection system (Bio-Rad) and normalized against expression of *PEX4* (*AT5G25760*) and *PP2A* (*AT1G13320*). Three technical replicates were performed for each independent biological replicate. The primers used are listed in Table S1. The samples for RNA-seq were harvested and the Illumina sequencing and analysis were performed as previously described (Sang *et al.*, 2020).

Scanning electron microscopy

Shoot apices were dissected, fixed and processed for scanning electron microscopy (SEM) as previously described (Laux *et al.*, 1996). Samples were dried in liquid carbon dioxide and mounted on stubs using double-sided adhesive and conductive tabs. Plant material was then coated with gold and platinum before imaging with a Supra 40VP scanning electron microscope (Zeiss). Meristems were imaged from directly above the meristem center.

In situ hybridization

In situ hybridization was performed as previously described (Bradley *et al.*, 1993) with minor modifications. Instead of Pronase, proteinase K (1 mg ml^{-1} in 100 mM Tris at pH 8.0, and 50 mM EDTA) was used for protease treatment and samples were incubated at 37°C for 30 min. Post-hybridization washes were performed in 0.1× saline sodium citrate with 50% (w/v) formamide. The sequences of primers to generate the probes of *AP2* mRNA are listed in Table S1. For the detection of mature miR172, the synthetic probe (osa-miR172a; Exiqon, Vedbaek, Denmark) was used (Hyun *et al.*, 2016). Three independent experiments including at least two meristems were analyzed for each genotype and time point. Representative images were presented.

Confocal microscopy

Shoot apices were harvested in ice-cold 4% paraformaldehyde (v/v) (Sigma-Aldrich) prepared in phosphate-buffered saline at pH 7.0. Samples were vacuum-infiltrated twice for 10 min each, transferred to fresh 4% paraformaldehyde, and stored at 4°C overnight. Fixed samples were washed in phosphate-buffered saline twice for 10 min each and cleared with ClearSee (Kurihara *et al.*, 2015) at room temperature for 3–7 d. Samples were then transferred to fresh ClearSee solution with 0.1% (v/v) SCRI Renaissance 2200 (Renaissance Chemicals, Selby, UK; Musielak *et al.*, 2015) and incubated in the dark overnight. Shoot meristems were imaged as described previously (Kinoshita *et al.*, 2020).

Image processing and analysis

Meristem area was quantified on SEM images by tracing a circle within the meristem that excluded the leaf primordia, using

Smart SEM (Zeiss). The divergence angle between the primordia within the SAM was measured on SEM images using FIJI. The center of the meristem was estimated by extracting the mean of the *XY* coordinates of the primordia. The measured angle was that formed by Primordium1-Centre-Primordium2. The number of cells within the meristem region and cell area were obtained using MORPHOGRAPHX (MGX) software (https://morphographx.org/; Kierzkowski *et al.*, 2012; Barbier de Reuille *et al.*, 2015). The Z-stack images were first converted into '.tif' images using FIJI and the surface of the acquired meristem was subsequently created with MGX. The signal of the cell wall (SCRI Renaissance 2200; 3–5 μm from the surface) was projected onto the surface and cells were autosegmented and manually corrected. The meristematic region was defined as described in Kinoshita *et al.* (2020). Cell area and cell distance from the central cell were computed with MGX. Different zones of the SAM were defined according to their position from the central cell (0): '0–2', included cells at positions 0–2 from the central cell corresponding to the CZ in Col-0; '3–5' contained cells at positions 3–5 from the central cell corresponding to the inner PZ; '6–8' included cells at positions 6–8 from the central cell corresponding to the middle of the PZ in Col-0; and '9–11' consisted of cells at positions 9–11 from the central cell corresponding to the outer part of the PZ. The VENUS fluorescence signals were quantified by tracing a circle of the same size for each image on the shoot meristem within primordia on the central transversal section using the SCRI Renaissance 2200 channel and measuring the mean gray value on the VENUS channel.

Statistical analysis

Data were analyzed using ANOVA followed by a *post hoc* Tukey's test using R software (http://r-project.org/). Flowering time data, total flower number, meristem area and fluorescence quantification are presented using boxplots: the boxes indicate the interquartile range, the horizontal line in the middle is the median, the vertical lines correspond to the highest or lowest value within 1.5 × the interquartile range. For each boxplot, single observations are presented as dots in the background.

Results

Expression patterns of miR172-sensitive and -resistant forms of AP2 at the shoot apex

In order to understand how AP2 responds to miR172 activity, we generated two transgenes expressing fusions between AP2 and the fluorescent protein VENUS from the endogenous regulatory sequences of *AP2* (Fig. S1a). To uncouple the activity of miR172 from AP2, we introduced synonymous mutations into the coding region of *AP2* to generate a miR172-resistant version of *AP2* (*pAP2::rAP2-VENUS*, later called *rAP2-VENUS*; Fig. S1a) (Chen, 2004). We transformed Col-0 plants with this *rAP2-VENUS* transgene and with a 'wild-type' version of the transgene that remained susceptible to miR172 activity (*pAP2::AP2-*
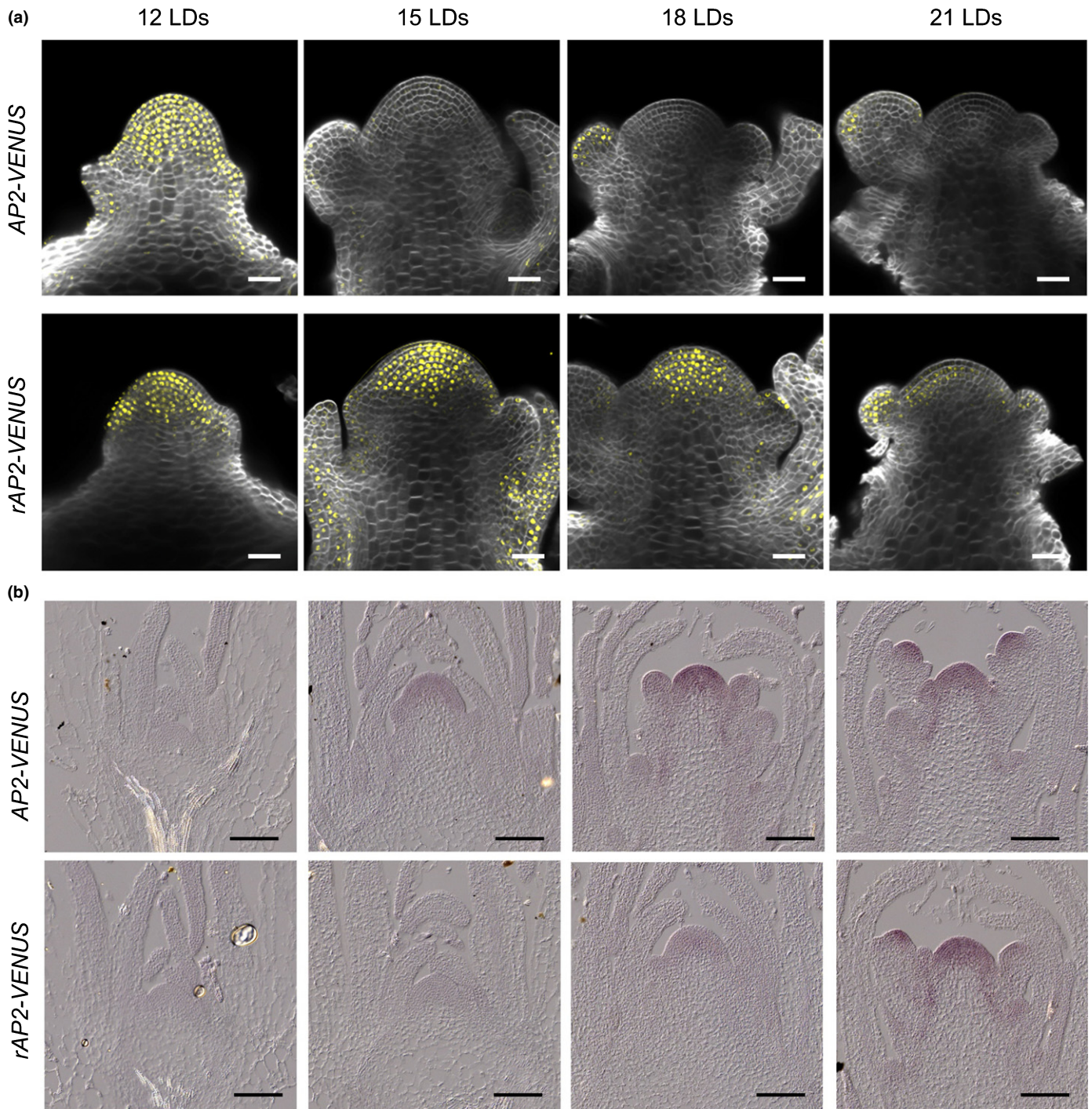
Fig. 1 miR172 decreases the level of AP2 in the shoot apical meristem (SAM) of *Arabidopsis thaliana* at floral transition. (a) Confocal imaging of *AP2-VENUS #13* and mutant variant *rAP2-VENUS #B3* transgenic lines grown under long-day (LD) conditions. Bar, 20 μm. (b) Detection of mature miR172 levels by *in situ* hybridization in the *AP2-VENUS #13* and mutant variant *rAP2-VENUS #B3* transgenic lines grown under LD conditions. Bar, 100 μm. LDs, number of days after germination under LD conditions.

VENUS, later called *AP2-VENUS*), which was partially described previously (Ó'Maoiléidigh *et al.*, 2021).

Several independent transformants for both constructs were analyzed for *AP2* mRNA level in seedlings and for VENUS expression in the SAM by confocal microscopy (Figs 1a, S1b,c). Most lines of the same genotype showed very similar patterns of expression, with the exception of line *AP2-VENUS #14*, which

showed a weaker VENUS signal (Figs 1a, S1b,c). Prior to floral development (12 LDs), AP-VENUS and rAP2-VENUS protein accumulated with similar spatial patterns in the SAM (Figs 1a, S1c). However, AP2-VENUS signal decreased with increasing plant age and was not detectable in the shoot meristem after 15 LDs (Figs 1a, S1d). By contrast, miR172 was not detected at the SAM by *in situ* hybridization at 12 LD but was clearly present at

15 LD, appearing to be anti-correlated with AP2 in the shoot meristem (Fig. 1b). In comparison to AP2-VENUS, the rAP2-VENUS fluorescence signal persisted in the SAM much longer and was still detected at 21 LDs (Fig. 1a). Interestingly, the accumulation of miR172 was delayed in *rAP2-VENUS* plants and was not detectable until 18 LDs, which may be an indirect effect of the late-flowering phenotype of *rAP2-VENUS* plants (see later). However, rAP2-VENUS signal did overlap with miR172 accumulation at 21 LDs in *rAP2-VENUS* plants (Fig. 1a,b), supporting the possibility that this transgene is resistant to miR172 activity. We monitored *AP2* mRNA localization in the SAM along a similar time course, and *AP2* transcripts were still detectable in the meristem of *AP2-VENUS* plants at 21 LDs when AP2-VENUS protein was undetectable, supporting the significance of post-transcriptional regulation of *AP2* at the SAM (Fig. S2). However, the pattern of rAP2-VENUS did become more restricted in the SAM between 18 and 21 LDs, indicating that other regulators control the abundance of AP2 independently of *MIR172* (Fig. 1a).

Analysis of flowering time and flower development in *AP2-VENUS* and *rAP2-VENUS* transgenic plants

AP2 was previously reported to delay floral transition under non-inductive SD and inductive LD photoperiods (Yant *et al.*, 2010; Ó'Maoiléidigh *et al.*, 2021). Consistent with these results, we observed that *ap2-12* mutants flowered earlier with fewer leaves and *AP2-VENUS* plants flowered slightly later with more leaves than Col-0 under both LDs and SDs (Figs 2a, S3a,b). By contrast, the flowering time of the two *rAP2-VENUS* lines tested was strongly delayed in both LD and SD conditions (Figs 2b, S3a,b), but this delay was more pronounced in SD conditions, in which *rAP2-VENUS* plants produced more than 160 rosette leaves (Fig. S3b). These results confirm that AP2 has a major role in repressing floral transition in SD conditions and demonstrate that inhibition of *AP2* activity by miR172 is required for timely flowering (Yant *et al.*, 2010; Ó'Maoiléidigh *et al.*, 2021).

The *AP2-VENUS* and *rAP2-VENUS* transgenes were introgressed into the *ap2-12* mutant background and the morphology and flowering time of these plants were assessed after verifying homozygosity of each mutation and transgene. The *AP2-VENUS* construct complemented the early flowering of *ap2-12* mutants, confirming the function of the fusion protein (Figs 2a, S3c). However, *rAP2-VENUS ap2-12* plants produced significantly more rosette leaves than did *rAP2-VENUS* plants (Fig. 2b), which may be due to impaired negative feedback regulation of AP2 at its own locus (Schwab *et al.*, 2005; Yant *et al.*, 2010). Furthermore, the *AP2-VENUS* transgene restored the aberrant floral morphology of *ap2-12* mutants, whereas *rAP2-VENUS* plants displayed defects in flower formation such as enlarged carpels (Fig. S3c).

Flower initiation rates are altered in an AP2-dependent manner

The inflorescences of *rAP2-VENUS* plants were compact and contained more flowers when compared with Col-0 control

plants (Fig. 2c). A large number of flowers developed from the primary shoot of *rAP2-VENUS* plants over their lifetime, whereas fewer developed from the primary shoot of *ap2-12* plants, as compared with Col-0 controls (Figs 2d, S3d). This increase in flower production by *rAP2-VENUS* plants does not appear to be explained by an increased production of infertile flowers (Hensel *et al.*, 1994), because *ap2-12* plants produced more infertile flowers than *rAP2-VENUS* from their primary shoots (Fig. 2d).

To distinguish between the role of AP2 in the rate of flower production and meristem arrest at the end of flowering (Balanzà *et al.*, 2018), we counted the number of flowers present every 2 d following the opening of the first flower (Fig. 2e). Under our conditions, we observed that Col-0 plants underwent meristem arrest at 17 d after the first open flower (Fig. 2e). The *rAP2-VENUS* plants produced significantly more flowers than Col-0 from 5 d after the first open flower until the end of the experiment (23 d after flowering; Fig. 2e). Therefore, increased AP2 activity caused an increase in the rate of flower production from very early stages of flowering and extended the duration of floral production. To independently assess the contribution of miR172 to an increased rate of flower production, we counted the number of flowers produced by *mir172abd* plants, which have severely reduced miR172 activity at the shoot apex (Ó'Maoiléidigh *et al.*, 2021). The *mir172abd* mutant produced flowers at a rate similar to *rAP2-VENUS* plants at early stages of flowering (up to 11 d after flowering) but produced fewer flowers than *rAP2-VENUS* plants overall (Fig. 2d,e). Both *rAP2-VENUS* transgenic lines tested showed the same flower-number phenotype (Fig. S3d), indicating that the difference between *mir172abd* and *rAP2-VENUS* in flower number is not specific to a single *rAP2-VENUS* transgene insertion.

To assess whether *mir172c* and *mir172e* account for the difference in flower production observed between *rAP2-VENUS* and *mir172abd*, the number of flowers produced by *mir172abcde* plants was also counted (Fig. S4). They produced a slightly higher number of flowers than *mir172abd* plants, but lower than that for *rAP2-VENUS* (Figs 2e, S4), which suggests that other miR172 targets might influence the increase in flower number observed in *mir172* plants. To validate this hypothesis, we also counted the number of flowers produced by *mir172abd ap2-12* plants. This genotype produced significantly fewer flowers than *mir172abd*, but slightly more than Col-0 (Fig. 2d). This indicates that the increased rate of flower production is largely dependent on AP2 with possible minor contributions from other miR172 targets late in the flowering phase. The rate of flower production by *mir172abd ap2-12* and *ap2-12* was similar until 23 d after the first open flower, suggesting that the role of miR172 in flower production before meristem arrest depends exclusively on AP2 (Fig. 2d,e).

The effect of AP2 and rAP2 on meristem size

The rate of organ initiation correlates with the size of the meristem, and larger meristems produce more organs per unit time (Je *et al.*, 2016; Serrano-Mislata *et al.*, 2017; Landrein *et al.*,
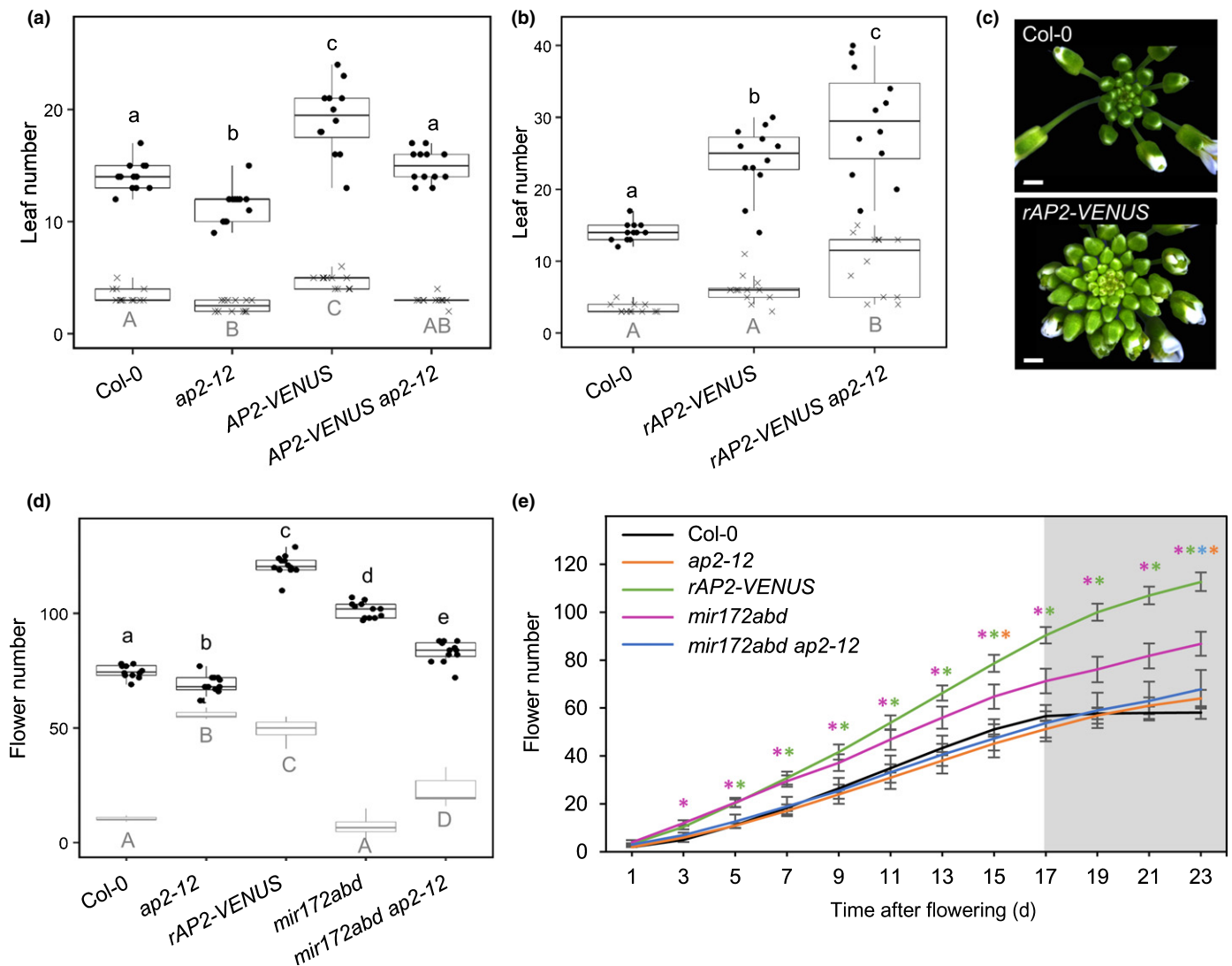
Fig. 2 AP2 accumulation after floral transition delays flowering and increases floral determinacy in *Arabidopsis thaliana*. (a) Number of rosette (gray) and total leaves (black) for Col-0, *ap2-12*, *AP2-VENUS #13* and *AP2-VENUS #13 ap2-12* ($n \geq 11$) plants. (b) Number of rosette (gray) and total leaves (black) for Col-0, *rAP2-VENUS #A6* and *rAP2-VENUS #A6 ap2-12* plants ($n \geq 11$). For (a, b), letters show significant differences between genotypes ($P < 0.05$, using ANOVA followed by Tukey's pairwise multiple comparisons). (c) Photographs of inflorescences of Col-0 (top) and *rAP2-VENUS #A6* (bottom) plants. Plants photographed 10 d after the first flower opened. Bar, 0.1 cm. (d) Total number of flowers (black) and infertile flowers (gray) on the primary inflorescence of Col-0, *ap2-12*, *rAP2-VENUS #A6*, *mir172abd* and *mir172abd ap2-12* plants. Letters show statistical grouping of genotypes ($n = 12$; $P < 0.05$, ANOVA followed by Tukey's pairwise multiple comparisons). (e) The cumulative number of mature flowers on the primary inflorescence (mean ± SD for 12 plants per genotype; day 1 was when the first flower opened); asterisks indicate $P < 0.05$ in comparisons between Col-0 and *ap2-12* (orange), *rAP2-VENUS #A6* (green), *mir172abd* (pink) or *mir172abd ap2-12* (blue) ($n = 12$; using ANOVA followed by Tukey's pairwise multiple comparisons). The gray square represents the stage at which the Col-0 plants underwent meristem arrest. In (a, b, d), whiskers represent a distance of 1.5 × interquartile range, the vertical line in the middle is the median, and the dots or crosses display individual data points.

2018). Therefore, we examined the inflorescence meristem sizes of Col-0, *rAP2-VENUS*, *mir172abd*, *ap2-12* and *mir172abd ap2-12* plants (Fig. 3), and compared meristem size of *AP2-VENUS* Col-0 with *rAP2-VENUS* Col-0, Col-0 and *ap2-12* (Fig. S5). To compare this parameter among plants with different flowering times, we harvested apices at the 1-cm-bolting stage. *rAP2-VENUS* plants exhibited larger meristems than Col-0 controls, whereas *ap2-12* meristems were smaller and *AP2-VENUS* meristems were similar to Col-0 (Figs 3a–c, S5). The meristem size of *mir172abd* plants was intermediate between that of Col-0 and *rAP2-VENUS* plants (Fig. 3c), which might

explain the observed differences in flower production (Fig. 2d). Moreover, the meristem area of *mir172abd ap2-12* plants was similar to that of *ap2-12* (Fig. 3c), demonstrating that AP2 is required for the enlarged meristem phenotype. Importantly, this result demonstrates that inflorescence meristem size is not correlated with flowering time in these genotypes, because *mir172abd ap2-12* plants flower later than Col-0 (Ó'Maoiléidigh *et al.*, 2021), but their inflorescence meristem is smaller than Col-0. Collectively, these results suggest that a strong correlation exists between meristem area and the rate of flower production among these genotypes.

To identify the cellular mechanism responsible for the difference in meristem size among these genotypes, we analyzed the cell number and cell area in the L1 of their inflorescence meristems (Fig. 3a). The mean number of cells in the *ap2-12* meristem was 176, compared with 370 in Col-0 at the 1-cm-bolting stage (Fig. 3d). This reduced cell number was compensated by a significant increase in cell size throughout the entire meristematic region in *ap2-12* meristems (Fig. 3e,f). The same phenotype was observed for the meristems of *mir172abd ap2-12* plants, suggesting that AP2 is the key regulator of meristem morphology downstream of miR172. In addition to an increase in cell number, cell area was significantly greater in the meristem of the *rAP2-VENUS* plants, but only in the zones close to the central part of the meristem (0–2, 3–5 and 6–8 cells from the central cell) and not in the region close to the meristem boundary (9–11 cells from the central cell; Fig. 3e,f). Likewise, in the *mir172abd* meristem, cells were larger than Col-0 in the same zones (0–2, 3–5 and 6–8 cells from the central cell) but cell number in the meristem was similar to the one observed in Col-0 meristems (Fig. 3a–d).

Variation in meristem size is correlated with changes in phyllotaxy (Landrein *et al.*, 2014), and we therefore tested the hypothesis that a shorter plastochron affects the divergence angle of primordium formation in the shoot meristem. Although a significant difference in meristem area was observed for the majority of the genotypes tested, a significantly smaller angle between successive primordia was only observed in *rAP2-VENUS* plants (Fig. 3g). This suggests that a large difference in SAM size is required to affect the phyllotactic divergence angle. Collectively, these results show that an extended duration of AP2 expression in the SAM after floral transition in *rAP2-VENUS* plants was associated with a larger meristem due to an increase in both cell number and area.

AP2 and ARF3 coordinately control inflorescence meristem size and flower initiation rate

We showed that miR172 represses AP2-VENUS expression at the shoot apex during floral transition, which reduces the size of the inflorescence meristem (Figs 1a, 3). Within the floral meristem, AP2 binds to and reduces transcription of *ARF3*, also known as *ETTIN* (Liu *et al.*, 2014), while in inflorescence samples, ARF3 also directly negatively regulates *AP2* transcription, creating a double-negative feedback loop (Simonini *et al.*, 2017). ARF3 protein accumulates throughout the inflorescence meristem (Liu *et al.*, 2014; Simonini *et al.*, 2017) and mutation of *ARF3* leads to larger floral and inflorescence meristems (Zhang *et al.*, 2018). Consistent with this report, we observed that the meristem of *arf3-2* was larger than that of Col-0 at the 1-cm-bolting stage (Fig. 4a–c). This increase in meristem area was explained by a significant increase in cell area specifically in the outer part of the PZ (6–8 and 9–11 cells from the central cell; Fig. 4a,e,f).

To determine whether the regulation of meristem size by AP2 depends on ARF3, we measured the meristem area of the *ap2-12 arf3-2* mutant. The size of the *ap2-12 arf3-2* meristem was intermediate between that of *ap2-12* and *arf3-2*, and similar to that of

Col-0 (Fig. 4c). We then examined the effect of *arf3-2* mutation in the *rAP2-VENUS* background and observed that the meristem area of *rAP2-VENUS arf3-2* plants was significantly larger than that of *rAP2-VENUS* (Fig. 4c). This increase in meristem size was sufficient to decrease the divergence angle between primordia at the SAM (Fig. 4g). These results indicate that reduction of *ARF3* transcription might contribute to the role of AP2 in regulating meristem size, but it does not fully explain it. Furthermore, although cell area in *rAP2-VENUS* increased in the central part of the meristem and cell area in *arf3-2* increased in the meristem periphery, the cell area in *rAP2-VENUS arf3-2* increased in all regions, as compared with Col-0 (Fig. 4f). These results suggest that AP2 and ARF3 regulate cell area in the SAM via different mechanisms, but the regulation of cell number is consistent with *AP2* being negatively regulated by ARF3.

To test the interaction between AP2 and ARF3 further, we quantified *AP2* expression in the shoot apex of *arf3-2* at the 1-cm-bolting stage, and observed a slight but not significant reduction of *AP2* expression in *arf3-2* from the wild-type expression level (Fig. S5a). Because AP2 binds directly to the *ARF3* locus (Yant *et al.*, 2010), we also quantified the accumulation of *ARF3* mRNA in *ap2-12* and *rAP2-VENUS* shoot apices, but observed almost no difference in expression compared with that in Col-0 (Fig. S5b). *ARF3* and *AP2* may be regulated differently in floral meristems than in the inflorescence meristem, so we examined the accumulation of the rAP2-VENUS protein in *rAP2-VENUS arf3-2* plants that showed a larger meristem than *rAP2-VENUS* plants. Quantification of VENUS signal specifically in the SAM showed that it was stronger in the *rAP2-VENUS arf3-2* meristem than in the *rAP2-VENUS* meristem (Fig. 5a–c). These data suggest that ARF3 may fine-tune AP2 expression level to contribute to the regulation of meristem size.

We next examined whether the change in meristem size of *arf3-2* affected floral bud production. The number of flowers and the rate of bud production were significantly higher for *arf3-2* than for Col-0 (Fig. 6). The number of flowers produced began to differ significantly from Col-0 from 13 d after the opening of the first flower, suggesting that *arf3-2* regulates flower production during the early stages of flowering (Fig. 6b). Similar to the intermediate size of the meristem observed in *ap2-12 arf3-2*, the number of flowers was also intermediate between the one of *ap2-12* and *arf3-2* and was similar to that in Col-0 (Fig. 6a). A similar number of flowers was produced by the primary inflorescences of *rAP2-VENUS arf3-2* and *rAP2-VENUS* plants. The shoot meristem sizes between these plants were also very similar, although *rAP2-VENUS arf3-2* meristems were slightly larger. However, this phenotype might have been affected by the increased sterility of the *rAP2-VENUS arf3-2* plants (Fig. 6a). We conclude that ARF3 regulates meristem size and flower production partially through different pathways.

Expression of rAP2 in the central zone strongly affects inflorescence meristem size

To identify in which areas of the meristem rAP2 influences shoot meristem size, the effects of rAP2 expression in different domains
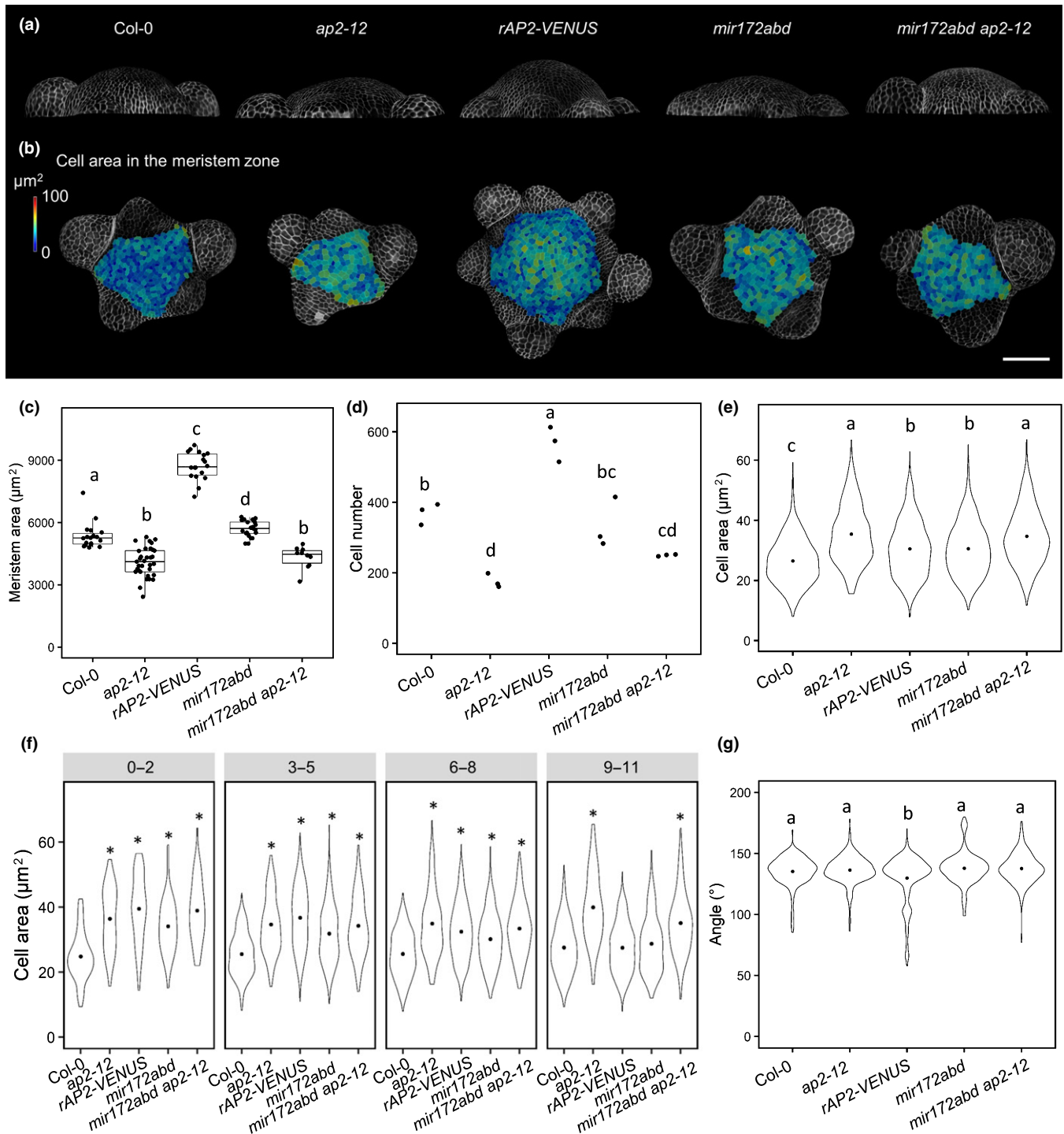
Fig. 3 miR172 mediates the regulation of inflorescence meristem size by AP2 in *Arabidopsis thaliana*. (a, b) The shoot apical meristem (SAM) of Col-0, *ap2-12, rAP2-VENUS #A6, mir172abd* and *mir172abd ap2-12* plants at the 1-cm-bolting stage observed from the side (a), and heat map quantification of the cell area in the meristem region observed from the top (b). Cell wall signals in the L1 were projected onto the surface of the meristem. Bar, 50 μm. (c) Meristem area as determined by scanning electron microscopy (SEM) analysis ($n \geq 12$). (d, e) Cell number (d) and cell area (e) in the meristem region ($n = 3$) of Col-0, *ap2-12, rAP2-VENUS #A6, mir172abd* and *mir172abd ap2-12* plants at the 1-cm-bolting stage. Letters show significant differences between genotypes ($P < 0.05$, using ANOVA followed by Tukey's pairwise multiple comparisons). (f) Cell area in different zones of the meristem of Col-0, *ap2-12, rAP2-VENUS #A6, mir172abd* and *mir172abd ap2-12* plants at the 1-cm-bolting stage. Meristem zones are determined by the distance in cells from the centre of the meristem: 0–2 cells, 3–5 cells, 6–8 cells, 9–11 cells. Asterisks indicate $P < 0.05$ between comparisons of Col-0 and other genotypes using ANOVA followed by pairwise multiple comparisons using Tukey's test. (g) The divergence angle between primordia at the SAM of Col-0, *ap2-12, rAP2-VENUS #A6, mir172abd* and *mir172abd ap2-12* plants at the 1-cm-bolting stage. Letters show statistical groupings for genotypes ($n \geq 12$; $P < 0.05$, using ANOVA followed by Tukey's pairwise multiple comparisons). In (c), whiskers represent a distance of 1.5 × interquartile range, the vertical line in the middle is the median, and the dots display individual data points. In (e–g), the dot in the middle is the mean.
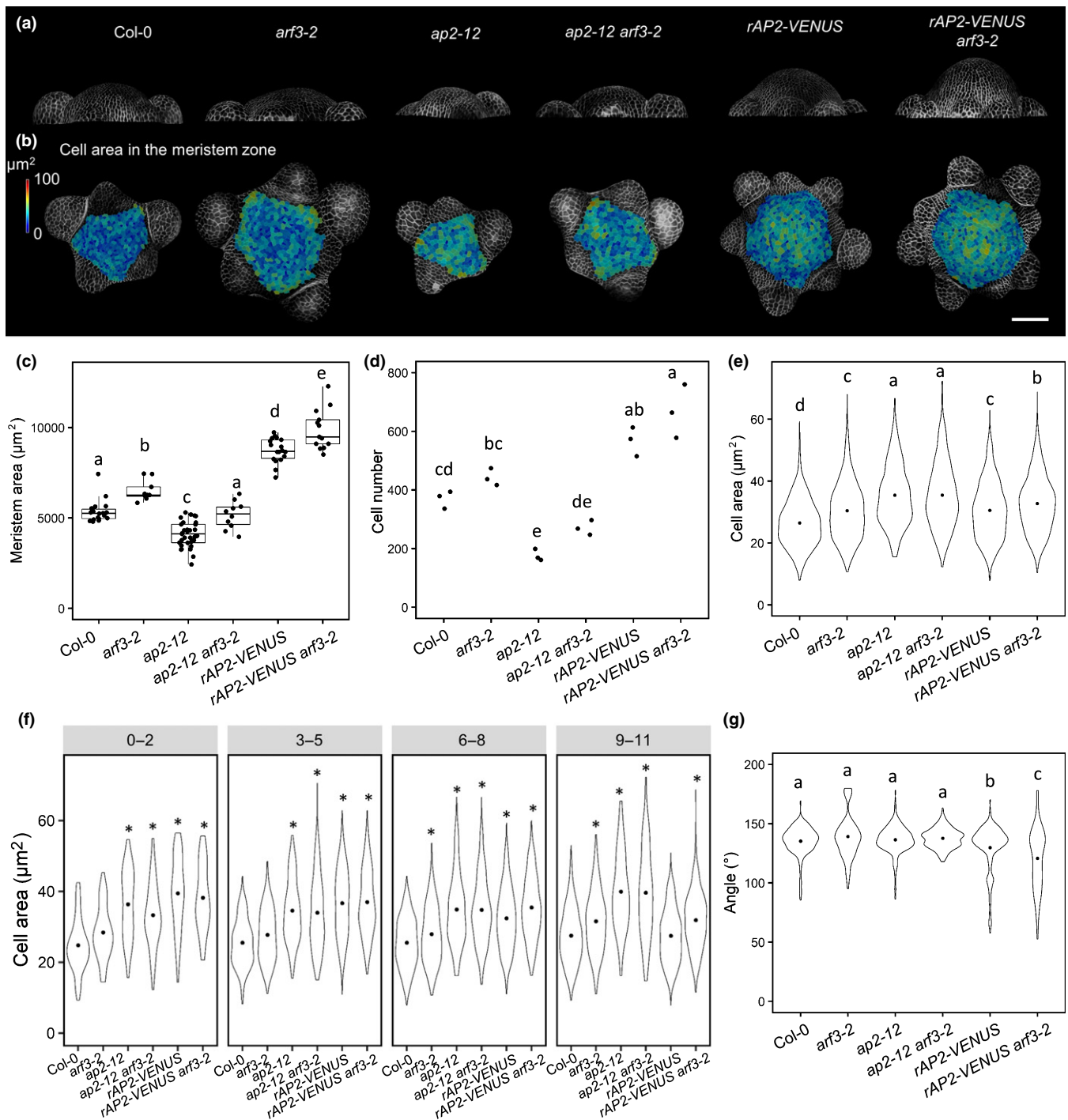
Fig. 4 AP2 and ARF3 regulate cell size in different meristem zones in *Arabidopsis thaliana*. (a, b) The shoot apical meristem (SAM) of Col-0, *arf3-2*, *ap2-12*, *ap2-12 arf3-2*, *rAP2-VENUS #A6* and *rAP2-VENUS #A6 arf3-2* plants at the 1-cm-bolting stage observed from the side (a), and heat map quantification of the cell area in the meristem region observed from the top (b). Cell wall signals in the L1 were projected onto the surface of the meristem. Bar, 50 μm. (c–e) Meristem area as determined by scanning electron microscopy (SEM) analysis ($n \geq 9$) (c), cell number (d) and cell area in the meristem region ($n = 3$) (e) of Col-0, *arf3-2*, *ap2-12*, *ap2-12 arf3-2*, *rAP2-VENUS #A6* and *rAP2-VENUS #A6 arf3-2* plants at the 1-cm-bolting stage. Letters show statistical grouping of genotypes ($P < 0.05$, using ANOVA followed by Tukey's pairwise multiple comparisons). (f) Cell area of different zones of the meristem of Col-0, *arf3-2*, *ap2-12*, *ap2-12 arf3-2*, *rAP2-VENUS #A6* and *rAP2-VENUS #A6 arf3-2* plants at the 1-cm-bolting stage. Meristem zones are determined by the distance in cells from the centre of the meristem: 0–2 cells, 3–5 cells, 6–8 cells, 9–11 cells. Asterisks indicate $P < 0.05$ between the genotypes tested and Col-0 (using ANOVA followed by Tukey's pairwise multiple comparisons). (g) Divergence angle between primordia at the SAM of Col-0, *arf3-2*, *ap2-12*, *ap2-12 arf3-2*, *rAP2-VENUS #A6* and *rAP2-VENUS #A6 arf3-2* plants at the 1-cm-bolting stage. Letters show statistical groupings for genotypes ($n \geq 9$; $P < 0.05$, using ANOVA followed by Tukey's pairwise multiple comparisons). Images and data for Col-0, *ap2-12* and *rAP2-VENUS #A6* are the same as those in Fig. 3. In (c), whiskers represent a distance of 1.5 × interquartile range, the vertical line in the middle is the median, and the dots display individual data points. In (e–g), the dot in the middle is the mean.
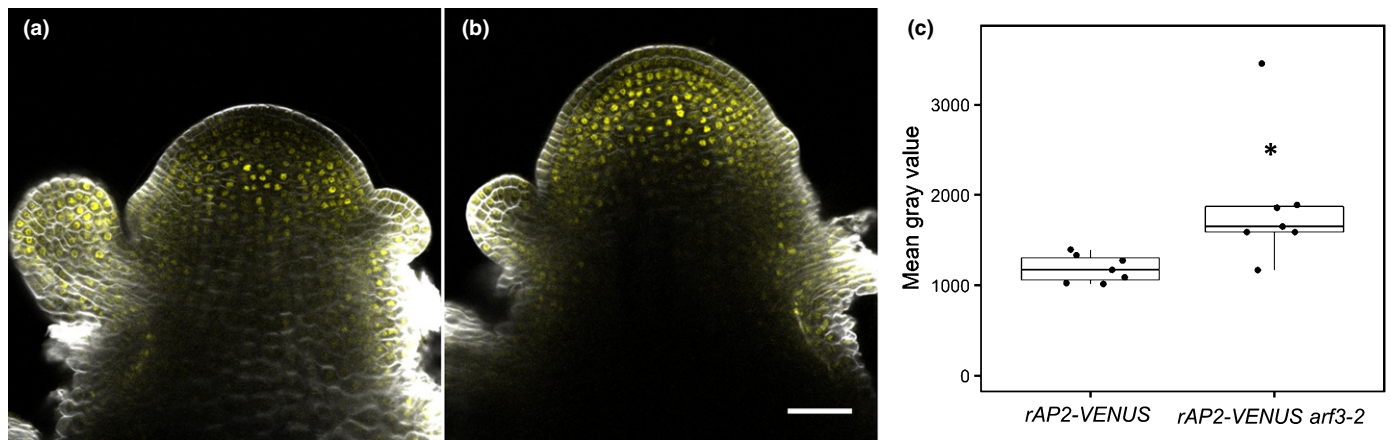
Fig. 5 Genetic interaction between AP2 and ARF3 in the inflorescence meristem of *Arabidopsis thaliana* at the 1-cm-bolting stage. (a–c) Confocal imaging (a, b) and fluorescence quantification (c) of rAP2-VENUS in *rAP2-VENUS #A6* (a) and *rAP2-VENUS #A6 arf3-2* (b) in inflorescence meristems at the 1-cm-bolting stage ($n \geq 7$). Bar, 25 μm; asterisks show $P < 0.05$ between genotypes using ANOVA followed by Tukey's pairwise multiple comparisons. In (c), whiskers represent a distance of 1.5 × interquartile range, the vertical line in the middle is the median, and the dots display individual data points.

of the SAM was analyzed. The *FD* promoter was used to mark cells in the whole SAM, because it is strongly expressed in the SAM, as well as in the adaxial epidermis of young leaf primordia (Abe *et al.*, 2005; Wigge *et al.*, 2005; Romera-Branchat *et al.*, 2020). The *A. thaliana MERISTEM LAYER 1* (*AtML1*) promoter was used to drive *rAP2-VENUS* expression in the L1 layer of the meristematic region and differentiating organs (Lu *et al.*, 1996), and the *HIGH MOBILITY GROUP* promoter (*pHMG*) was used to express *rAP2-VENUS* in the L1 of the shoot meristem (Yadav *et al.*, 2014). Furthermore, the *WUS* (Mayer *et al.*, 1998) and *CLV3* promoters (Yadav *et al.*, 2009) were used to express *rAP2-VENUS* in the OZ and CZ, respectively. Fusions of

rAP2-VENUS to these different promoters were introduced into Col-0. *AP2* acts as a floral-organ patterning gene (Bowman *et al.*, 1989; Krogan *et al.*, 2012), and most of the transgenic plants were infertile, except for *pCLV3::rAP2-VENUS*.

The T1 generation was analyzed and in all T1 plants that carried the *pAtML1::rAP2-VENUS* or *pHMG::rAP2-VENUS* transgene, the fusion protein was localized as expected in the L1 cells of the SAM at floral transition (14 LDs) and in the L1 of the SAM and of the floral primordia in the mature inflorescence (21 LDs; Fig. 7a,b). Expression of *rAP2-VENUS* in the L1 affected neither meristem size (Fig. 7c) nor the number of flowers (Fig. 7d), whereas in *pFD::rAP2-VENUS* transgenic plants,
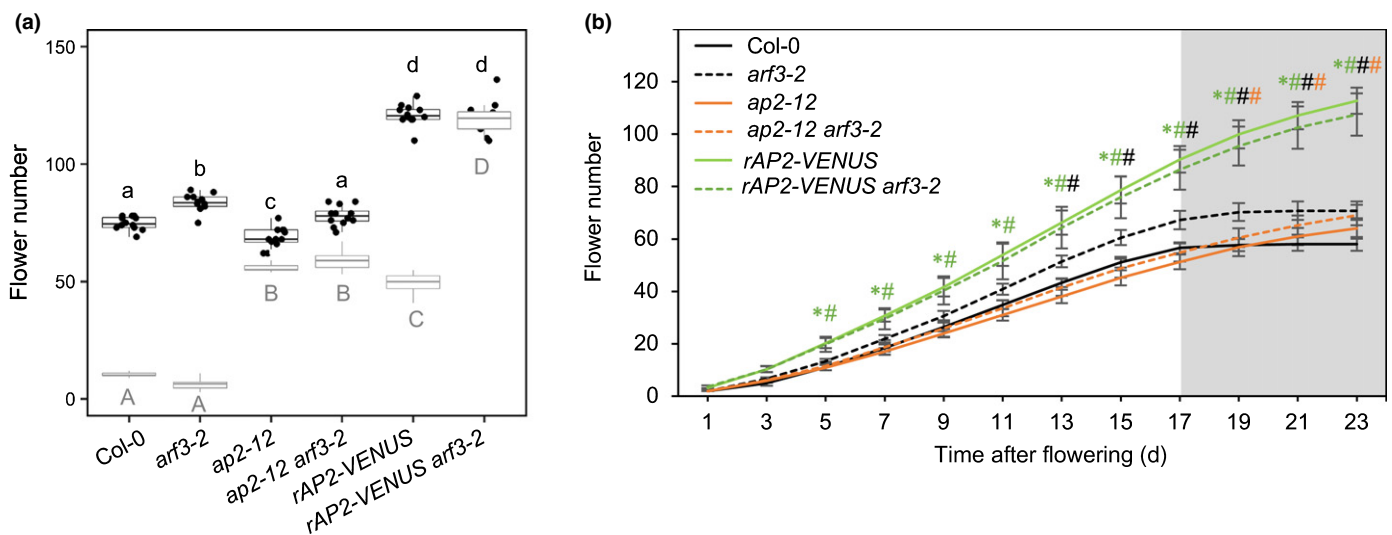

Fig. 6 ARF3 regulates floral determinacy in *Arabidopsis thaliana*. (a, b) Total number of flowers (black) and infertile flowers (gray) on the primary inflorescence (a) and cumulative number of mature flowers on the primary inflorescence (mean ± SD for 12 plants per genotype; day 1 was when the first flower was opened) (b). Letters show statistical groupings of genotypes ($P < 0.05$, using ANOVA followed by Tukey's pairwise multiple comparisons). Asterisks indicate significant differences between Col-0 and *ap2-12* (orange) or *rAP2-VENUS #A6* (green) using ANOVA followed by Tukey's pairwise multiple comparisons. Hashtags indicate significant differences between Col-0 and *arf3-2* (black), *ap2-12 arf3-2* (orange) or *rAP2-VENUS #A6 arf3-2* (green) using ANOVA followed by Tukey's pairwise multiple comparisons ($n = 12$). Data for Col-0, *ap2-12* and *rAP2-VENUS #A6* are the same as those in Fig. 2d,e. In (a), whiskers represent a distance of 1.5 × interquartile range, the vertical line in the middle is the median, and the dots display individual data points.
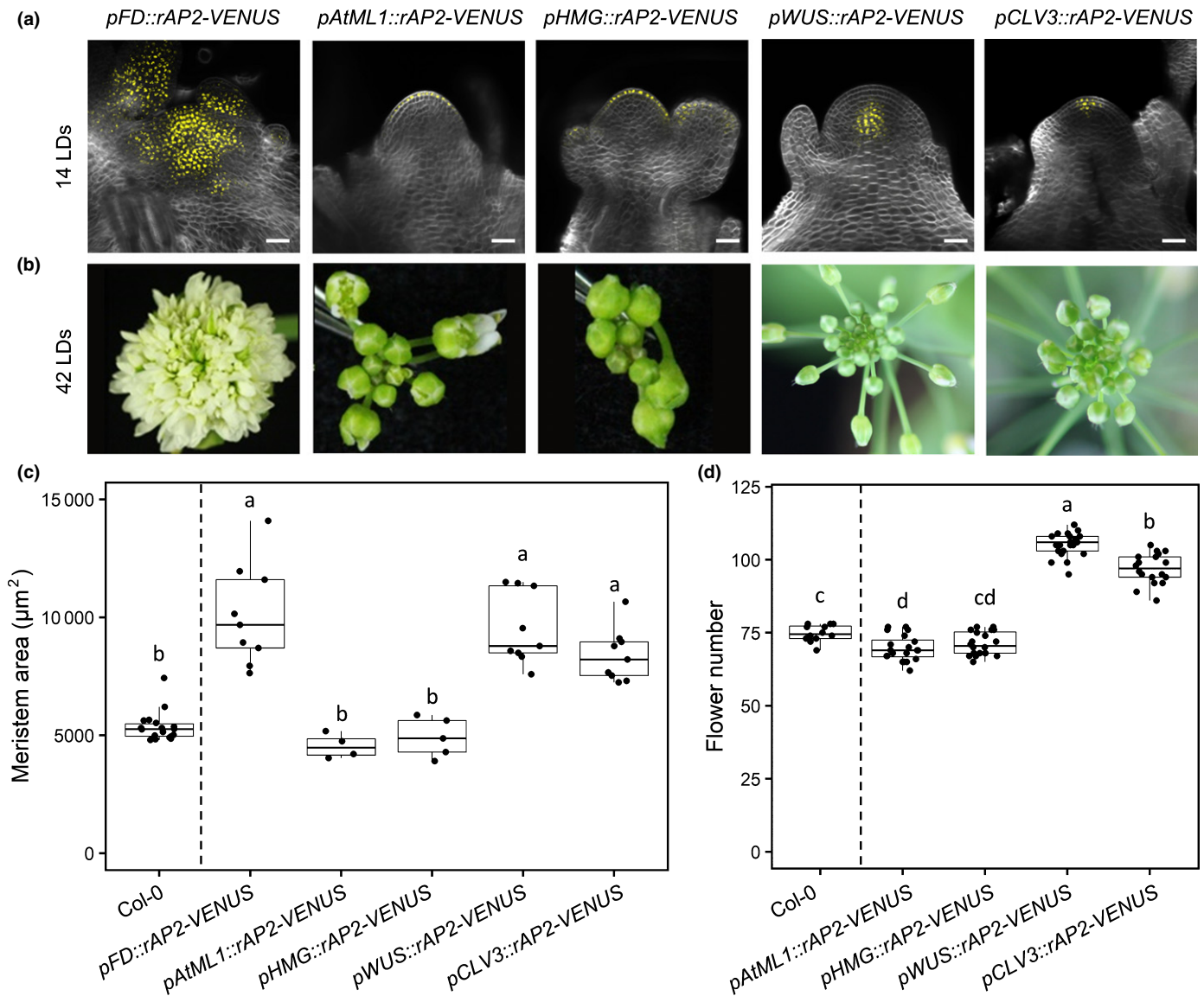
Fig. 7 In *Arabidopsis thaliana* AP2 regulates inflorescence meristem size and flower determinacy mainly in the central zone. (a) Confocal microscopy analysis of *pFD::rAP2-VENUS*, *pAtML1::rAP2-VENUS*, *pHMG::rAP2-VENUS*, *pWUS::rAP2-VENUS* and *pCLV3::rAP2-VENUS* plants under long-day (LD) conditions. The number of plants of each genotype analyzed were eight, four, five, nine and nine, respectively. Bar, 20 µm. LDs, number of days after germination under LD conditions. (b) Inflorescences of *pFD::rAP2-VENUS*, *pAtML1::rAP2-VENUS*, *pHMG::rAP2-VENUS*, *pWUS::rAP2-VENUS* and *pCLV3::rAP2-VENUS* plants grown for 42 LDs. (c, d) Inflorescence meristem area as determined by confocal microscopy ($n \geq 4$) (c) and number of flowers on the primary shoot of *pAtML1::rAP2-VENUS*, *pHMG::rAP2-VENUS*, *pWUS::rAP2-VENUS* and *pCLV3::rAP2-VENUS* plants ($n \geq 18$) (d). The Col-0 plants were analyzed in a separate experiment without BASTA selection and are shown to indicate the expected meristem area and flower number of a wild-type control. Letters show statistical groupings of genotypes ($P < 0.05$, using ANOVA followed by Tukey's pairwise multiple comparisons). In (c, d), whiskers represent a distance of 1.5 × interquartile range, the vertical line in the middle is the median, and the dots display individual data points.

rAP2-VENUS accumulated throughout the SAM and meristem size was significantly increased, to a level similar to that observed for *pAP2::rAP2-VENUS* (Figs 7, 3c). Flower morphology was severely disrupted in *pAtML1::rAP2-VENUS* plants and flowers of *pHMG::rAP2-VENUS* transformants contained more petals and stamens than did Col-0 (Fig. S6d,e). This result suggests that the expression of *rAP2-VENUS* in the L1 affects floral morphology but not meristem size. *pFD::rAP2-VENUS* plants also showed strong defects in flower formation (Fig. 7b). All of the *pFD::rAP2-VENUS* T1 plants tested produced more cauline leaves, were delayed in producing flowers and the inflorescence terminated in a highly enlarged floral structure consisting mainly of petals (Figs 7b, S6c,f, S7g). In *pWUS::rAP2-VENUS* and *pCLV3::rAP2-VENUS* transformants, rAP2-VENUS localized to the OC and the CZ, respectively, as expected (Fig. 7a,b). *pWUS::rAP2-VENUS* and *pCLV3::rAP2-VENUS* plants formed larger meristems than did Col-0, which appeared similar in size to those of *pFD::rAP2-VENUS* plants (Fig. 7c), and had formed floral primordia by 21 d after sowing, indicating that they were not as strongly delayed in floral transition as *pFD::rAP2-VENUS* (Fig. S7g). Although rAP2-VENUS increased meristem size when expressed in the *WUS* or *CLV3* domains, no difference in

the level or spatial patterns of expression of *WUS* or *CLV3* mRNA were detected in inflorescence meristems of *AP2::rAP2-VENUS* plants by *in situ* hybridization or RNA-seq (Fig. S8). Furthermore, analysis of the expression domain of *WUS::NLS-VENUS* (Pfeiffer *et al.*, 2016) in Col-0 and *rAP2* plants indicated that the *WUS* domain was broader in *rAP2* meristems but that it increased proportionately with the rest of the meristem (Fig. S9). In conclusion, expression of *rAP2-VENUS* in distinct domains suggests that the CZ- and OC-specific expression of AP2 contributes to its role in determining meristem size, but the increase in inflorescence meristem size does not appear to be caused by a disproportionate increase in the size of these domains.

Discussion

We showed that miR172-mediated regulation of *AP2* is important for controlling inflorescence meristem size by modulating cell size and number. We also found that the role of ARF3 in regulating meristem size is partially dependent on AP2 activity but that it also has distinct functions at the shoot apex. Moreover, detailed morphological analysis of various mutants revealed that AP2 and ARF3 influence cell morphology in overlapping and spatially distinct regions. Misexpression of *rAP2* confirmed that the activity of AP2 in the CZ and OC strongly increases shoot meristem size. Collectively, these demonstrate the importance of the miR172/ AP2 module in regulating inflorescence meristem size.

Repression of AP2 by miR172 in the SAM regulates flowering time

Plants harboring a miR172-resistant version of *AP2* (*rAP2-VENUS*) flowered later than the Col-0 wild-type and plants carrying a miR172-susceptible version of *AP2* (*AP2-VENUS*) in both inductive and noninductive photoperiods. Plants that expressed *AP2-VENUS* in an *ap2-12* background flowered at a similar time to the Col-0 wild-type, demonstrating that the transgene effectively complements the *ap2-12* mutation. Interestingly, *rAP2-VENUS ap2-12* plants flowered later than *rAP2-VENUS* Col-0. This difference may be due to the autoregulatory feedback loop in which AP2 inhibits its own transcription (Schwab *et al.*, 2005; Yant *et al.*, 2010). In Col-0 plants, mutual repression of each other's transcription by AP2 and rAP2 will result in a pool of *AP2* mRNA that is both sensitive and insensitive to miR172, whereas in *rAP2-VENUS ap2-12* the total pool of *AP2* mRNA will be resistant to miR172. This feedback loop is further complicated by the influence of AP2 on the accumulation of miR172, which we found to be delayed in *rAP2-VENUS* plants compared with Col-0. The precise mechanism that underlies this delay is unknown, but it may be partially due to the transcriptional repression of *MIR172B* by AP2 (Yant *et al.*, 2010). The characterization and modeling of the interactions between members of the group of six *AP2-LIKE* and five *MIR172* genes will deepen our understanding of how the mRNAs of transcription factors are regulated by miRNAs in plants.

The rAP2-VENUS protein continues to accumulate at the shoot apex beyond floral transition, whereas AP2-VENUS expression rapidly decreases in the shoot apex once miR172 activity increases in the inflorescence meristem. Although rAP2-VENUS expression persists longer than that of AP2-VENUS, the level of rAP2-VENUS is gradually depleted in the inflorescence meristem independently of miR172 sensitivity. This reduction is correlated with an increase in the level of the *FRUITFULL* (*FUL*) transcription, which encodes a MADS-box transcription factor that directly represses *AP2* transcription (Balanzà *et al.*, 2018). Plants that lack miR172 and FUL activity display phenotypes similar to those resulting from *AP2* overexpression (Ó'Maoiléidigh *et al.*, 2021), which is consistent with the repression of *AP2* transcription by FUL.

Accumulation of AP2 in the SAM after floral transition leads to an increase in meristem area

Meristem size is one of the aspects of Arabidopsis development influenced by AP2. We observed that *ap2-12* mutants possessed smaller inflorescence meristems than did Col-0 controls, which is consistent with previous observations (Würschum *et al.*, 2006). By contrast, *rAP2-VENUS* plants had much larger meristems than did the wild-type, which was largely explained by an increase in cell number in the meristematic region. We also observed that the meristem size of *mir172abd* plants was larger than that of the Col-0 control, consistent with recently published results (Lian *et al.*, 2021). Notably, the meristem sizes of *mir172abd ap2-12* and *ap2-12* were similar, indicating that AP2 is the only miR172 target with a strong effect on meristem size. Also, this demonstrates that AP2 has a role in determining inflorescence size independently of flowering time, because *mir172abd ap2-12* and *ap2-12* have similarly sized inflorescence meristems, but *mir172abd ap2-12* flowers much later than *ap2-12* (Ó'Maoiléidigh *et al.*, 2021). However, the meristem area of *rAP2-VENUS* plants was much larger than that of the *mir172abd* mutant. Although other miR172 targets do not regulate meristem size, their increased levels in the *mir172abd* background might reduce *AP2* transcription, leading to a lower level of AP2 in the *mir172abd* background than in *rAP2-VENUS*, which would therefore explain the difference in meristem size observed between *rAP2-VENUS* and *mir172abd*.

We analyzed the morphology of cells in the L1 of the meristematic region of several genotypes, including *ap2-12* and *rAP2-VENUS*, and observed an increase in mean cell area in the SAM of all genotypes. Because we analyzed only the morphology of cells in the L1, changes observed in this cell layer may originate from additional morphological modifications in the inner cell layers. To examine this further, we misexpressed *rAP2-VENUS* from a variety of tissue-specific promoters. Notably, expression of *rAP2-VENUS* specifically in the L1 layer did not affect meristem size, but expression of *rAP2-VENUS* in the CZ or OC substantially increased meristem size. These data suggest that the changes in cell number and area observed in the L1 of *rAP2-VENUS* plants are an effect of rAP2 activity deeper within the meristem.

The mRNA of the homeodomain transcription factor WUS localizes to the OC, and WUS is essential for maintenance of the stem cell population (Laux *et al.*, 1996; Mayer *et al.*, 1998).

Ectopic expression of *WUS* in the CZ can promote expansion of this region and increase the rate of cell division in the peripheral zone (Yadav *et al.*, 2010). AP2 regulates *WUS* expression in both shoot apical and floral meristems, albeit indirectly (Würschum *et al.*, 2006; Zhao *et al.*, 2007; Balanzà *et al.*, 2018). Thus, accumulation of rAP2-VENUS protein in the SAM may, in consequence, increase cell proliferation. It has previously been shown that modification of cell cycle activity at the SAM leads to changes in mean cell area in the L1 (Jones *et al.*, 2017). The increase in cell proliferation in the *rAP2-VENUS* meristem may therefore lead to an increase in cell area. In addition, the length of the cell cycle appears to change in order to maintain cell size homeostasis (Serrano-Mislata *et al.*, 2017). These compensatory mechanisms may lead to an increase in cell size in a tissue in which cell proliferation is enhanced or reduced, as observed for *rAP2-VENUS* and *ap2-12*, respectively. The first changes in cellular behavior caused by rAP2 in the meristem could be explored in future experiments using inducible gene fusions, as has been done for other meristematic regulators (Caggiano *et al.*, 2017).

AP2 regulates meristem size in the CZ and OC, whereas ARF3 functions specifically in the PZ

ARF3 is a direct target gene of AP2 that regulates SAM area (Yant *et al.*, 2010; Zhang *et al.*, 2018). The ARF3 transcription factor mediates functions of AGAMOUS (AG), AP2 and the phytohormone cytokinin to regulate *WUS* expression in the floral meristem (Liu *et al.*, 2014; Zhang *et al.*, 2018).

To describe AP2 regulation by ARF3 in the SAM in more detail, we observed rAP2-VENUS localization in the *arf3-2* plants and concluded that the absence of ARF3 protein increased the amount of rAP2-VENUS, consistent with previous results (Simonini *et al.*, 2017). Therefore, ARF3 limits the accumulation of AP2, potentially as part of a mechanism that facilitates the development of different regions of the shoot apex (e.g. CZ vs PZ).

By contrast to *ap2-12* mutants, the SAM of *arf3-2* is larger in area compared with Col-0. The meristem size of *ap2-12 arf3-2* plants was intermediate between that of *ap2-12* and *arf3-2*, suggesting that AP2 and ARF3 transcription factors regulate cell proliferation at the SAM independently. We observed that ARF3 regulates cell size in the PZ, whereas rAP2 regulates cell size in the CZ and OC. Consistent with this, ectopic expression of *ARF3* in the CZ from the *CLV3* promoter did not cause an altered meristem phenotype (Ma *et al.*, 2019), whereas *pCLV3::rAP2-VENUS* induced a large increase in meristem size. Therefore, we conclude that AP2 and ARF3 regulate cell proliferation at the SAM in at least partially nonoverlapping zones. Notably, *ARF3* was recently identified to be a putative target of WUS (Ma *et al.*, 2019), adding another degree of complexity to the gene regulatory network that regulates SAM size.

AP2 and its downstream targets are promising candidates to improve yield in crops

In addition to a significant increase in meristem size observed in *rAP2-VENUS* plants, they also displayed a higher rate of flower production. AP2 controls flower number in Arabidopsis through modulating the timing of meristem arrest (Balanzà *et al.*, 2018). We observed an increase in flower production prior to the onset of meristem arrest in *rAP2-VENUS* and *mir172abd* plants that was associated with an increase in meristem size and was similar to the phenotypes observed in *della* and *ckx3 ckx5* mutants (Bartrina *et al.*, 2011; Serrano-Mislata *et al.*, 2017). A positive correlation between flower production and meristem size has also been observed for different Arabidopsis ecotypes (Landrein *et al.*, 2014) and in response to nutrient deficiency (Landrein *et al.*, 2018). Phenotypic analysis of all genotypes tested in this study indicated that there was a correlation between flower number and meristem area (Fig. S10).

Modification of AP2 activity may be useful for plant breeding, despite its pleiotropic effects on development. Although most plants in which *AP2* was ectopically expressed were infertile, *pCLV3::rAP2-VENUS* plants were not only fertile, but also formed large SAMs and produced more flowers than wild-type plants. This observation may be relevant for crops because functions of AP2-like transcription factors are conserved across monocotyledons and dicotyledons (Zhu & Helliwell, 2011). In maize (*Zea mays*), *INDETERMINATE SPIKELET1* (*IDS1*) and *SISTER OF INDETERMINATE SPIKELET1* (*SID1*) encode AP2-like transcription factors that are required for branching of the inflorescence meristem, to initiate floral meristems and to control spikelet meristem determinacy. Both gene products are targets of TASSELSEED4 (TS4), which encodes a miR172 isoform (Chuck *et al.*, 1998, 2007, 2008). In rice (*Oryza sativa*), the *AP2-like* genes *SUPERNUMERARY BRACT* (*SNB*) and *OsINDETERMINATE SPIKELET 1* (*OsIDS1*) influence inflorescence architecture and floral meristem establishment, and transcription of both genes is repressed by overexpression of miR172 (Lee *et al.*, 2007; Lee & An, 2012). In wheat (*Triticum* spp.), the *rAP2L-A5* allele is resistant to miR172 cleavage, which affects shoot meristem determinacy (Debernardi *et al.*, 2017; Greenwood *et al.*, 2017). *INTERMEDIUM-M* encodes an HvAP2L-H5 ortholog and is required for inflorescence indeterminacy and spikelet determinacy in barley (Zhong *et al.*, 2021). Overall, miR172 and its target genes perform crucial roles in floral transition, flower development and shoot meristem maintenance, which are relatively well conserved between monocots and eudicots. This study shows that modification of AP2 activity represents a feasible approach to increase meristem size, flower number and seed production, and a better understanding of the mechanisms underlying this control may contribute to improvement of crop productivity.

Acknowledgements

Author contributions

QS, AV and GC designed the experiments, initiated the project and wrote the manuscript. QS, AV, DSO'M, XY, CV, EBGdO, MC and RF conducted the experiments. QS and AV contributed equally.

ORCID

Enric Bertran Garcia de Olalla (iD) https://orcid.org/0000-0003-2987-1849
Martina Cerise (iD) https://orcid.org/0000-0002-9654-252X
George Coupland (iD) https://orcid.org/0000-0001-6988-4172
Diarmuid S. Ó'Maoiléidigh (iD) https://orcid.org/0000-0002-3043-3750
Qing Sang (iD) https://orcid.org/0000-0003-1163-1521
Alice Vayssières (iD) https://orcid.org/0000-0002-8625-2879
Coral Vincent (iD) https://orcid.org/0000-0002-9696-2639
Xia Yang (iD) https://orcid.org/0000-0002-8142-5857

Data availability

The data that support the findings of this study are available from the corresponding author upon reasonable request. The RNA-seq data are available from the NCBI Gene Expression Omnibus (GEO) under accession no. GSE196925.

References

Abe M, Kobayashi Y, Yamamoto S, Daimon Y, Yamaguchi A, Ikeda Y, Ichinoki H, Notaguchi M, Goto K, Araki T. 2005. FD, a bZIP protein mediating signals from the floral pathway integrator FT at the shoot apex. *Science* 309: 1052–1056.

Aukerman MJ, Sakai H. 2003. Regulation of flowering time and floral organ identity by a microRNA and its APETALA2-Like target genes. *Plant Cell* 15: 2730–2741.

Balanzà V, Martínez-Fernández I, Sato S, Yanofsky MF, Kaufmann K, Angenent GC, Bemer M, Ferrándiz C. 2018. Genetic control of meristem arrest and life span in Arabidopsis by a FRUITFULL-APETALA2 pathway. *Nature Communications* 9: 565.

Barbier de Reuille P, Routier-Kierzkowska A-L, Kierzkowski D, Bassel GW, Schüpbach T, Tauriello G, Bajpai N, Strauss S, Weber A, Kiss A *et al.* 2015. MorphoGraphX: a platform for quantifying morphogenesis in 4D. *eLife* 4: 1–20.

Bartrina I, Otto E, Strnad M, Werner T, Schmülling T. 2011. Cytokinin regulates the activity of reproductive meristems, flower organ size, ovule formation, and thus seed yield in *Arabidopsis thaliana. Plant Cell* 23: 69–80.

Bowman JL, Smyth DR, Meyerowitz EM. 1989. Genes directing flower development in Arabidopsis. *Plant Cell* 1: 37–52.

Bradley D, Carpenter R, Sommer H, Hartley N, Coen E. 1993. Complementary floral homeotic phenotypes result from opposite orientations of a transposon at the *plena* locus of Antirrhinum. *Cell* 72: 85–95.

Caggiano MP, Yu XL, Bhatia N, Larsson A, Ram H, Ohno C, Sappl P, Meyerowitz EM, Jonsson H, Heisler MG. 2017. Cell type boundaries organize plant development. *eLife* 6: e27421.

Carles CC, Fletcher JC. 2003. Shoot apical meristem maintenance: the art of a dynamic balance. *Trends in Plant Science* 8: 394–401.

Chen X. 2004. A microRNA as a translational repressor of APETALA2 in Arabidopsis flower development. *Science* 303: 2022–2025.

Chuck G, Meeley RB, Hake S. 1998. The control of maize spikelet meristem fate by the APETALA2-like gene indeterminate spikelet1. *Genes and Development* 12: 1145–1154.

Chuck G, Meeley R, Irish E, Sakai H, Hake S. 2007. The maize tasselseed4 microRNA controls sex determination and meristem cell fate by targeting Tasselseed6/indeterminate spikelet1. *Nature Genetics* 39: 1517–1521.

Chuck G, Meeley R, Hake S. 2008. Floral meristem initiation and meristem cell fate are regulated by the maize AP2 genes ids1 and sid1. *Development* 135: 3013–3019.

Chung CT, Niemela SL, Miller RH. 1989. One-step preparation of competent *Escherichia coli*: transformation and storage of bacterial cells in the same solution. *Proceedings of National Academy of Sciences USA* 86: 2172–2175.

Clark SE, Running MP, Meyerowitz EM. 1993. CLAVATA1, a regulator of meristem and flower development in Arabidopsis. *Development* 119: 397–418.

Clark SE, Running MP, Meyerowitz EM. 1995. CLAVATA3 is a specific regulator of shoot and floral meristem development affecting the same processes as CLAVATA1. *Development* 121: 2057–2067.

Clark SE, William RW, Meyerowitz EM. 1997. The *CLAVATA1* gene encodes a putative receptor kinase that controls shoot and floral meristem size in Arabidopsis. *Cell* 89: 575–585.

Clough SJ, Bent AF. 1998. Floral dip: a simplified method for *Agrobacterium*-mediated transformation of *Arabidopsis thaliana*. *The Plant Journal* 16: 735–743.

Debernardi JM, Lin H, Chuck G, Faris JD, Dubcovsky J. 2017. microRNA172 plays a crucial role in wheat spike morphogenesis and grain threshability. *Development* 144: 1966–1975.

Fletcher JC, Brand U, Running MP, Simon R, Meyerowitz EM. 1999. Signaling of cell fate decisions by CLAVATA3 in Arabidopsis shoot meristems. *Science* 283: 1911–1914.

Greenwood JR, Finnegan EJ, Watanabe N, Trevaskis B, Swain SM. 2017. New alleles of the wheat domestication gene Q reveal multiple roles in growth and reproductive development. *Development* 144: 1959–1965.

Hensel LL, Nelson MA, Richmond TA, Bleecker AB. 1994. The fate of inflorescence meristems is controlled by developing fruits in Arabidopsis. *Plant Physiology* 106: 863–876.

Holt AL, van Haperen JMA, Groot EP, Laux T. 2014. Signaling in shoot and flower meristems of *Arabidopsis thaliana*. *Current Opinion in Plant Biology* 17: 96–102.

Hyun Y, Coupland G, Martinez-Gallegos R, Porri A, Richter R, Vincent C. 2016. Multi-layered regulation of SPL15 and cooperation with SOC1 integrate endogenous flowering pathways at the Arabidopsis shoot meristem. *Developmental Cell* 37: 254–266.

Jacqmard A, Gadisseur I, Bernier G. 2003. Cell division and morphological changes in the shoot apex of *Arabidopsis thaliana* during floral transition. *Annals of Botany* 91: 571–576.

Je BI, Gruel J, Lee YK, Bommert P, Arevalo ED, Eveland AL, Wu Q, Goldshmidt A, Meeley R, Bartlett M *et al.* 2016. Signaling from maize organ primordia via FASCIATED EAR3 regulates stem cell proliferation and yield traits. *Nature Genetics* 48: 785–791.

Jones AR, Forero-Vargas M, Withers SP, Smith RS, Traas J, Dewitte W, Murray JAH. 2017. Cell-size dependent progression of the cell cycle creates homeostasis and flexibility of plant cell size. *Nature Communications* 8: 1–13.

Jung J-H, Seo Y-H, Seo PJ, Reyes JL, Yun J, Chua N-H, Park C-M. 2007. The GIGANTEA-regulated microRNA172 mediates photoperiodic flowering independent of CONSTANS in Arabidopsis. *Plant Cell* 19: 2736–2748.

Kierzkowski D, Nakayama N, Routier-Kierzkowska AL, Weber A, Bayer E, Schorderet M, Reinhardt D, Kuhlemeier C, Smith RS. 2012. Elastic domains regulate growth and organogenesis in the plant shoot apical meristem. *Science* 335: 1096–1099.

Kinoshita A, Vayssières A, Richter R, Sang Q, Roggen A, Van Driel AD, Smith RS, Coupland G. 2020. Regulation of shoot meristem shape by photoperiodic signaling and phytohormones during floral induction of Arabidopsis. *eLife* 9: 1–29.

Kitagawa M, Jackson D. 2019. Control of meristem size. *Annual Review of Plant Biology* 70: 269–291.

New
Phytologist

Klock HE, Lesley SA. 2009. The polymerase incomplete primer extension (PIPE) method applied to high-throughput cloning and site-directed mutagenesis. *Methods in Molecular Biology* **498**: 91–103.

Krogan NT, Hogan K, Long JA. 2012. APETALA2 negatively regulates multiple floral organ identity genes in Arabidopsis by recruiting the co-repressor TOPLESS and the histone deacetylase HDA19. *Development* **139**: 4180–4190.

Kurihara D, Mizuta Y, Sato Y, Higashiyama T. 2015. CLEARSEE: a rapid optical clearing reagent for whole-plant fluorescence imaging. *Development* **142**: 4168–4179.

Landrein B, Formosa-Jordan P, Malivert A, Schuster C, Melnyk CW, Yang W, Turnbull C, Meyerowitz EM, Locke JCW, Jönsson H. 2018. Nitrate modulates stem cell dynamics in Arabidopsis shoot meristems through cytokinins. *Proceedings of the National Academy of Science, USA* **115**: 1382–1387.

Landrein B, Refahi Y, Besnard F, Hervieux N, Mirabet V, Boudaoud A, Vernoux T, Hamant O. 2014. Meristem size contributes to the robustness of phyllotaxis in Arabidopsis. *Journal of Experimental Botany* **66**: 1317–1324.

Laux T. 2003. The stem cell concept in plants: a matter of debate. *Cell* **113**: 281–283.

Laux T, Mayer KFX, Berger J, Jürgens G, Genetik L, München L. 1996. The WUSCHEL gene is required for shoot and floral meristem integrity in Arabidopsis. *Development* **122**: 87–96.

Lee DY, An G. 2012. Two AP2 family genes, SUPERNUMERARY BRACT (SNB) and OsINDETERMINATE SPIKELET 1 (OsIDS1), synergistically control inflorescence architecture and floral meristem establishment in rice. *The Plant Journal* **69**: 445–461.

Lee DY, Lee J, Moon S, Park SY, An G. 2007. The rice heterochronic gene SUPERNUMERARY BRACT regulates the transition from spikelet meristem to floral meristem. *The Plant Journal* **49**: 64–78.

Lenhard M, Laux T. 2003. Stem cell homeostasis in the Arabidopsis shoot meristem is regulated by intercellular movement of CLAVATA3 and its sequestration by CLAVATA1. *Development* **130**: 3163–3173.

Lian H, Wang L, Ma N, Zhou C-M, Han L, Zhang T-Q, Wang J-W. 2021. Redundant and specific roles of individual MIR172 genes in plant development. *PLoS Biology* **19**: e3001044.

Liu X, Dinh TT, Li D, Shi B, Li Y, Cao X, Guo L, Pan Y, Jiao Y, Chen X. 2014. AUXIN RESPONSE FACTOR 3 integrates the functions of AGAMOUS and APETALA2 in floral meristem determinacy. *The Plant Journal* **80**: 629–641.

Lu P, Porat R, Nadeau JA, O'Neill SD. 1996. Identification of a meristem L1 layer-specific gene in Arabidopsis that is expressed during embryonic pattern formation and defines a new class of homeobox genes. *Plant Cell* **8**: 2155–2168.

Ma Y, Miotk A, Šutiković Z, Ermakova O, Wenzl C, Medzihradszky A, Gaillochet C, Forner J, Utan G, Brackmann K et al. 2019. WUSCHEL acts as an auxin response rheostat to maintain apical stem cells in Arabidopsis. *Nature Communications* **10**: 1–11.

Mathieu J, Yant LJ, Mürdter F, Küttner F, Schmid M. 2009. Repression of flowering by the miR172 Target SMZ. *PLoS Biology* **7**: e1000148.

Mayer K, Schoof H, Haecker A, Lenhard M, Jürgens G, Laux T. 1998. Role of *WUSCHEL* in regulating stem cell fate in the Arabidopsis shoot meristem. *Cell* **95**: 805–815.

Meyerowitz EM. 1997. Genetic control of cell division patterns in developing plants. *Cell* **88**: 299–308.

Murashige T, Skoog F. 1962. A revised medium for rapid growth and bio assays with tobacco tissue cultures. *Physiologia Plantarum* **15**: 473–497.

Musielak TJ, Schenkel L, Kolb M, Henschen A, Bayer M. 2015. A simple and versatile cell wall staining protocol to study plant reproduction. *Plant Reproduction* **28**: 161–169.

Nagai T, Ibata K, Park ES, Kubota M, Mikoshiba K, Miyawaki A. 2002. A variant of yellow fluorescent protein with fast and efficient maturation for cell-biological applications. *Nature Biotechnology* **20**: 1585–1588.

Ó'Maoiléidigh DS, van Driel AD, Singh A, Sang Q, Le Bec N, Vincent C, de Olalla EBG, Vayssières A, Romera Branchat M, Severing E et al. 2021. Systematic analyses of the *MIR172* family members of Arabidopsis define their distinct roles in regulation of APETALA2 during floral transition. *PLoS Biology* **19**: e3001043.

Okushima Y, Overvoorde PJ, Arima K, Alonso JM, Chan A, Chang C, Ecker JR, Hughes B, Lui A, Nguyen D et al. 2005. Functional genomic analysis of the AUXIN RESPONSE FACTOR gene family members in *Arabidopsis thaliana*: unique and overlapping functions of ARF7 and ARF19. *Plant Cell* **17**: 444–463.

Pfeiffer A, Janocha D, Dong Y, Medzihradszky A, Schöne S, Daum G, Suzaki T, Forner J, Langenecker T, Rempel E et al. 2016. Integration of light and metabolic signals for stem cell activation at the shoot apical meristem. *eLife* **5**: e17023.

Rhoades MW, Reinhart BJ, Lim LP, Burge CB, Bartel B, Bartel DP. 2002. Prediction of plant MicroRNA targets. *Cell* **110**: 513–520.

Rojo E, Sharma VK, Kovaleva V, Raikhel NV, Fletcher JC. 2002. CLV3 is localized to the extracellular space, where it activates the Arabidopsis CLAVATA stem cell signaling pathway. *Plant Cell* **14**: 969–977.

Romera-Branchat M, Severing E, Pocard C, Ohr H, Vincent C, Née G, Martinez-Gallegos R, Jang S, Andrés F, Madrigal P et al. 2020. Functional divergence of the Arabidopsis florigen-interacting bZIP transcription factors FD and FDP. *Cell Reports* **31**: 107717.

Sang Q, Pajoro A, Sun H, Song B, Yang X, Stolze SC, Andres F, Schneeberger K, Nakagami H, Coupland G. 2020. Mutagenesis of a quintuple mutant impaired in environmental responses reveals roles for CHROMATIN REMODELING4 in the Arabidopsis floral transition. *Plant Cell* **32**: 1479–1500.

Satina S, Blakeslee AF, Avery AG. 1940. Demonstration of the three germ layers in the shoot apex of datura by means of induced polyploidy in periclinal chimeras. *American Journal of Botany* **27**: 895.

Schmid M, Uhlenhaut NH, Godard F, Demar M, Bressan R, Weigel D, Lohman JU. 2003. Dissection of floral induction pathways using global expression analysis. *Development* **130**: 6001–6012.

Schwab R, Palatnik JF, Riester M, Schommer C, Schmid M, Weigel D. 2005. Specific effects of microRNAs on the plant transcriptome. *Developmental Cell* **8**: 517–527.

Serrano-Mislata A, Bencivenga S, Bush M, Schiessl K, Boden S, Sablowski R. 2017. DELLA genes restrict inflorescence meristem function independently of plant height. *Nature Plants* **3**: 749–754.

Simonini S, Bencivenga S, Trick M, Østergaard L. 2017. Auxin-induced modulation of ETTIN activity orchestrates gene expression in Arabidopsis. *Plant Cell* **29**: 1864–1882.

Stone JM, Trotochaud AE, Walker JC, Clark SE. 1998. Control of meristem development by CLAVATA1 receptor kinase and kinase-associated protein phosphatase interactions. *Plant Physiology* **117**: 1217–1225.

Wigge PA, Kim MC, Jaeger KE, Busch W, Schmid M, Lohmann JU, Weigel D. 2005. Integration of spatial and temporal information during floral induction in Arabidopsis. *Science* **309**: 1056–1059.

Würschum T, Groß-Hardt R, Laux T. 2006. APETALA2 regulates the stem cell niche in the Arabidopsis shoot meristem. *Plant Cell* **18**: 295–307.

Yadav RK, Girke T, Pasala S, Xie M, Reddy GV. 2009. Gene expression map of the Arabidopsis shoot apical meristem stem cell niche. *Proceedings of the National Academy of Sciences, USA* **106**: 4941–4946.

Yadav RK, Tavakkoli M, Reddy GV. 2010. WUSCHEL mediates stem cell homeostasis by regulating stem cell number and patterns of cell division and differentiation of stem cell progenitors. *Development* **137**: 3581–3589.

Yadav RK, Tavakkoli M, Xie M, Girke T, Venugopala RG. 2014. A high-resolution gene expression map of the Arabidopsis shoot meristem stem cell niche. *Development* **141**: 2735–2744.

Yant L, Mathieu J, Dinh TT, Ott F, Lanz C, Wollmann H, Chen X, Schmid M. 2010. Orchestration of the floral transition and floral development in Arabidopsis by the bifunctional transcription factor APETALA2. *Plant Cell* **22**: 2156–2170.

Zhang B, Wang L, Zeng L, Zhang C, Ma H. 2015. Arabidopsis TOE proteins convey a photoperiodic signal to antagonize CONSTANS and regulate flowering time. *Genes and Development* **29**: 975–987.

Zhang K, Wang R, Zi H, Li Y, Cao X, Li D, Guo L, Tong J, Pan Y, Jiao Y et al. 2018. AUXIN RESPONSE FACTOR3 regulates floral meristem determinacy by repressing cytokinin biosynthesis and signaling. *Plant Cell* **30**: 324–346.

Zhao L, Kim Y, Dinh TT, Chen X. 2007. miR172 regulates stem cell fate and defines the inner boundary of APETALA3 and PISTILLATA expression domain in Arabidopsis floral meristems. *The Plant Journal* **51**: 840–849.

Zhong J, Van EGW, Bi X, Lan T, Walla A, Sang Q, Franzer R, von Korff M. 2021. INTERMEDIUM-M encodes an HvAP2L-H5 ortholog and is required for inflorescence indeterminacy and spikelet determinacy in barley. *Proceedings of the National Academy of Sciences, USA* **118**: e2011779118.

Zhu QH, Helliwell CA. 2011. Regulation of flowering time and floral patterning by miR172. *Journal of Experimental Botany* **62**: 487–495.

Supporting Information

Additional Supporting Information may be found online in the Supporting Information section at the end of the article.

Fig. S1 Characterization of *AP2-VENUS* and *rAP2-VENUS* lines.

Fig. S2 *AP2* localization of *AP2-VENUS* and *rAP2-VENUS* in the shoot apex.

Fig. S3 Phenotyping characterization of *AP2-VENUS* and *rAP2-VENUS* lines.

Fig. S4 Number of flowers in *mir172abd* and *mir172abcde*.

Fig. S5 Comparison of inflorescence meristem area of AP2-VENUS Col-0 and rAP2-VENUS Col-0 at the 1-cm-bolting stage.

Fig. S6 Genetic interaction between *AP2* and *ARF3* in the SAM at the 1-cm-bolting stage.

Fig. S7 Plant and floral phenotypes resulting from *rAP2* misexpression in different regions of the shoot apex.

Fig. S8 *CLV3* and *WUS* expression in Col-0, *ap2-12* and *rAP2-VENUS*.

Fig. S9 *WUS::NLS-VENUS* expression in Col-0 and *rAP2*.

Fig. S10 Correlative analysis of flower number and meristem area in Arabidopsis plants with altered AP2 and ARF3 level.

Table S1 Primers used in this study.

Please note: Wiley Blackwell are not responsible for the content or functionality of any Supporting Information supplied by the authors. Any queries (other than missing material) should be directed to the *New Phytologist* Central Office.